Published in final edited form as:
Traffic. 2008 July ; 9(7): 1218–1231. doi:10.1111/j.1600-0854.2008.00752.x.

Rab14 Regulates Apical Targeting in Polarized Epithelial Cells

Khameeka N. Kitt[1,†], **Delia Hernández-Deviez**[†,2], **Sarah D. Ballantyne**[1], **Elias T. Spiliotis**[3], **James E. Casanova**[4], and **Jean M. Wilson**[1,*]

[1] Department of Cell Biology and Anatomy, Arizona Health Sciences Center, University of Arizona, PO Box 245044, Tucson, AZ 85724, USA

[3] Department of Biological Science, Stanford University, Stanford, CA 94305, USA

[4] Department of Cell Biology, University of Virginia Health System, Charlottesville, VA 22908, USA

Abstract

Epithelial cells display distinct apical and basolateral membrane domains, and maintenance of this asymmetry is essential to the function of epithelial tissues. Polarized delivery of apical and basolateral membrane proteins from the *trans* Golgi network (TGN) and/or endosomes to the correct domain requires specific cytoplasmic machinery to control the sorting, budding and fission of vesicles. However, the molecular machinery that regulates polarized delivery of apical proteins remains poorly understood. In this study, we show that the small guanosine triphosphatase Rab14 is involved in the apical targeting pathway. Using yeast two-hybrid analysis and glutathione S-transferase pull down, we show that Rab14 interacts with apical membrane proteins and localizes to the TGN and apical endosomes. Overexpression of the GDP mutant form of Rab14 (S25N) induces an enlargement of the TGN and vesicle accumulation around Golgi membranes. Moreover, expression of Rab14-S25N results in mislocalization of the apical raft-associated protein vasoactive intestinal peptide/MAL to the basolateral domain but does not disrupt basolateral targeting or recycling. These data suggest that Rab14 specifically regulates delivery of cargo from the TGN to the apical domain.

Keywords

apical targeting; epithelial cells; polarity; Rab14

Polarized membrane domains are a fundamental property of epithelial cells, imparting a functional surface asymmetry that is essential for vectorial transport of water, ions and solutes as well as for establishment of a barrier to pathogens. Establishment of cell polarity is triggered by cell–cell adhesion and proper sorting and recycling of proteins to membrane domains. To maintain these distinct apical and basolateral domains, newly synthesized and recycling membrane proteins must be delivered to the correct membrane domains, and this polarized delivery is critical for preserving the functional polarized state throughout the life of the cell (1,2).

Segregation of apical or basolateral proteins for delivery to the plasma membrane occurs in the *trans* Golgi network (TGN) or in endosomes (2). Basolateral targeting is known to be mediated by cytoplasmic signals through adaptor protein (AP)-1B adaptor-dependent (3–5) or -independent pathways (3,6). However, the signals involved in apical targeting comprise many

*Corresponding author: Jean M. Wilson, jeanw@email.arizona.edu.
†These authors contributed equally to this work.
[2]Current address: Institute for Molecular Bioscience, University of Queensland, Brisbane, Queensland 4072, Australia

Supplemental materials are available as part of the online article at http://www.blackwell-synergy.com

different forms. Apical signals have been linked to *N*- and *O*-glycosyl chains (7,8), glycosyl-phosphatidylinositol (GPI) moieties (9) and cytoplasmic domains (10–12). In addition, partitioning into glycolipid rafts, association with the MAL proteolipid [vasoactive intestinal peptide (VIP)17] and association with the phosphatidylinositol-4-phosphate-binding adaptor protein (FAPP2) have also been implicated in sorting of proteins and lipids destined for apical membranes (13–18).

When newly synthesized proteins or lipids arrive at the TGN or endosomes, they must partition into distinct membrane domains, assemble into proper carriers and be delivered to the correct surface. Recent studies have made use of live cell imaging techniques to provide images of basolateral and apical vesicles segregating from the TGN and fusing with distinct domains (19,20). Genetic and biochemical analyses have shown that protein complexes act in series to regulate budding, docking and fusion to complete basolateral targeting (3,5,15,21–25). Despite intensive work in the field, the machinery that regulates budding and transport of apically directed vesicles is not well understood. Using yeast two-hybrid and glutathione S-transferase (GST) pull-down approaches, we have found that the small guanosine triphosphatase (GTPase) Rab14 is part of the regulatory machinery for apical targeting. Expression of the GDP mutant form of Rab14 in Madin–Darby canine kidney (MDCK) cells causes a change in the morphology of the TGN, an increase in vesicles surrounding the Golgi membrane and mistargeting of the apical membrane protein VIP/MAL. Moreover, live cell imaging shows that Rab14 vesicles are very dynamic and fuse with early endosomes and the plasma membrane. Our results indicate that Rab14 regulates apical trafficking from the TGN to apical endosomes in polarized cells.

Results

The small GTPase Rab14 interacts with an apical endosomal membrane protein

To identify machinery for delivery of apical proteins, we utilized an integral membrane glycoprotein, endotubin. Endotubin is a type I transmembrane protein that localizes to apical early endosomes (26). Two motifs on the short cytoplasmic domain are necessary and sufficient for delivery to the apical endosomal compartment (12,26) (Figure 1A); mutagenesis of the cytoplasmic domain results in mis-targeting to the basolateral membrane (12), and addition of the cytoplasmic domain onto a basolaterally directed protein results in retargeting to the apical plasma membrane (12). Using the endotubin cytoplasmic domain as the bait (Figure 1A), we screened a yeast two-hybrid library constructed from messenger RNA (mRNA) derived from neonatal rat intestinal epithelial cells. This screening resulted in the isolation of the amino-terminal fragment of the small GTPase Rab14. This interaction in the yeast two-hybrid system was confirmed by transformation of the bait and activating domain plasmids into yeast followed by mating (unpublished results).

To determine if the nucleotide state of Rab14 affects the ability to bind endotubin, we used a directed yeast two-hybrid approach. Full-length Rab14 wild type (wt) was isolated by polymerase chain reaction (PCR) and inserted into the prey plasmid to confirm the interaction with the entire molecule. Mating of cells expressing full-length Rab14-wt with cells expressing the endotubin cytoplasmic domain resulted in robust growth on quadruple dropout plates lacking leucine, tryptophan, histidine and adenine, indicating a strong interaction. Growth was also seen with the Rab14-GTP (Rab14-Q70L) and Rab14-GDP (Rab14-S25N) mutants (unpublished data), suggesting that the interaction is not nucleotide dependent.

To biochemically characterize the Rab14–endotubin interaction, we performed a GST pull down using full-length Rab14-wt, Rab14-Q70L or Rab14-S25N fused to GST. Rab14–GST fusion proteins were incubated with MDCK homogenates stably expressing full-length endotubin followed by immunoblotting against endotubin (Figure 1B). As in the yeast two-

hybrid analysis, the interaction of endotubin with Rab14 was observed with all Rab14 nucleotide states. There appeared to be a slight increase in endotubin binding to Rab14-wt–GST compared with the other forms, but this difference was not significant between experiments. As expected, we observed no interaction of Rab14-wt–GST with the basolateral protein, E-cadherin (Figure 1B).

To determine if Rab14 binds to other apical proteins, we examined the apical raft-associated protein, VIP/MAL. As shown in Figure 1C, Rab14-wt–GST pulled down VIP/MAL. Interestingly, in contrast with endotubin, no interaction was observed with Rab14-S25N–GST, suggesting that the interaction of Rab14 with VIP/MAL depends on the nucleotide state of Rab14 (Figure 1B). Again, we observed no interaction with the basolateral protein, E-cadherin (Figure 1C). These results further support the finding that Rab14 interacts specifically with apical proteins.

Previously, we showed that mutations in either the hydrophobic motif (F1180A) or the CKII site (T1186A) in the cytoplasmic domain of endotubin resulted in a small amount of basolateral missorting of this apical endosomal protein, although 90% was targeted apically (26). In contrast, mutation of both motifs resulted in 90% of endotubin being missorted to the basolateral domain (12). To determine if these two motifs are necessary for interaction with Rab14, we introduced the endotubin cytoplasmic domain mutants F1180A and T1186A into the yeast two-hybrid bait plasmid to test their ability to interact with Rab14. We found that yeast containing Rab14 and either of the endotubin cytoplasmic domain mutations (F1180A or T1186A) grew on selection medium, demonstrating a positive interaction (Table 1). However, the double mutant F1180A/T1186A does not show any interaction with Rab14 in the yeast two-hybrid system (Table 1). These results indicate that Rab14 does not interact with the basolaterally missorted endotubin mutant, suggesting that Rab14 plays a role in apical sorting and targeting of proteins in epithelial cells.

Because Rab14 was isolated as a result of its interaction with endotubin, we reasoned that these molecules would colocalize in the same compartment. First, we tested whether green fluorescent protein (GFP)-tagged Rab14 could be properly geranylgeranylated using Triton X-114 (TX-114) phase partitioning. Our results show that all the expressed forms of Rab14–GFP partitioned into the detergent pellet, indicating normal lipid modification (Figure S1). Next, we characterized the subcellular localization of Rab14 and endotubin in polarized MDCK cells. Coexpression of endotubin with Rab14-wt (Figure 1D, panel a) and Rab14-Q70L (Figure 1D, panel b) resulted in significant colocalization. We observe a decrease in colocalization between Rab14-S25N and endotubin (Figure 1D, panel c). Additionally, Rab14-wt and -Q70L together with endotubin localize to the apical cytoplasm. Because endotubin has been shown to be present in apical early endosomes, these results indicate that Rab14 is localizing to an apical early endosome compartment (26–28). This contrasts with the distribution of Rab14-S25N, which appears to be nonpolarized (Figure 1D, panel c).

Subcellular localization of Rab14 in polarized epithelial cells

To identify the subcellular compartment in which Rab14 functions, we examined the intracellular distribution of Rab14-wt–GFP in polarized and nonpolarized MDCK cells. Recent study in fibroblasts has shown that Rab14 localized to the biosynthetic pathway in both early and recycling endosomes (29) and to the phagosome in macrophages (30). As shown in Figure 2A, in polarized epithelial cells, Rab14-wt–GFP partially colocalizes with furin, an endogenous protein that recycles between the TGN and endosomes as AP-1A-dependent cargo (31). There was also partial colocalization of Rab14-wt–GFP with the common endosome marker, transferrin (Figure 2C). We observe no significant colocalization between Rab14-wt–GFP and the apical recycling endosome marker, Rab11a (Figure 2B), suggesting that Rab14 localizes to a distinct apical endosomal compartment.

Similarly, in nonpolarized MDCK cells grown on coverslips, we observe Rab14-wt–GFP and furin localizing to a perinuclear compartment (Figure 3A), but labeling is present in distinct, adjacent membrane domains (Figure 3A, panel a′). There was no significant colocalization between Rab14-wt–GFP and the AP-1 adaptor subunit γ-adaptin (Figure 3A, panel b′), suggesting that Rab14 predominantly traffics through a non-clathrin-dependent pathway. We also observe no colocalization between Rab14-wt–GFP and clathrin heavy chain, early embryonic antigen 1 (EEA1) or Golgi 58K (Figure S2). We observe limited areas of colocalization of Rab14-wt–GFP with the recycling endosomal marker transferrin in nonpolarized MDCK cells (Figure 3A, panel c′) but not with the lysosomal marker, Lysotracker (Figure S2). These results indicate that Rab14 is trafficking between the TGN, apical endosome (endotubin) and common endosome (transferrin) (28) and suggests that Rab14 may regulate trafficking between the Golgi and apical plasma membrane through different compartments depending on the polarized state of the cell (27).

As in nonpolarized cells (29), the nucleotide-binding state of Rab14 determines its subcellular localization in MDCK cells. Previous study has shown that the inactive form of Rab14 (Rab14-S25N) is localized in a predominantly perinuclear distribution. Labeling of the TGN with wheat germ agglutinin (WGA) (32) resulted in extensive colocalization with Rab14-S25N–GFP (Figure 3B, panel c). In addition, in cells expressing Rab14-S25N–GFP, the TGN was massively expanded and distorted, a morphology not seen with overexpression of the Rab14-wt–GFP (Figure 3B, panel a) or Rab14-Q70L–GFP (Figure 3B, panel b). This effect on the morphology of the TGN has also been reported by others in fibroblasts (29) and indicates that Rab14 may modulate fusion or exit of vesicles at the TGN. To determine if the distension of the TGN observed in Rab14-S25N–GFP caused an upregulation of synthesis of Golgi matrix and tether proteins, MDCK cell homogenates stably expressing Rab14-wt–GFP or Rab14-S25N–GFP were immunoblotted for Golgi proteins. However, there was no change in the steady-state amounts of these proteins (Figure S3).

The expansion of the TGN observed in Rab14-S25N–GFP-expressing cells suggests that there may be a block to budding from the TGN or an accumulation of vesicles in the peri-Golgi region. To determine this, we performed ultra-structural analysis on stably transfected MDCK cells expressing Rab14-wt–GFP or Rab14-S25N–GFP. The electron microscope (EM) images show dramatic phenotypic differences. Cells expressing Rab14-wt–GFP have normal Golgi morphology, with Golgi cisternae surrounded by budded vesicles (Figure 4A, left panel), as previously observed in NRK cells (29). Conversely, Rab14-S25N–GFP-expressing cells display larger and more distended Golgi cisternae (similar to Figure 3B, panel c) and an increase in vesicles accumulating in the vicinity of the Golgi stacks (Figure 4A, right panel).

Because we observe vesicles lining up at the Golgi membrane in Rab14-S25N–GFP-expressing cells (Figure 4C), we next determined if there was a block to vesicle fission by quantifying the number of unattached and attached vesicles in the peri-Golgi region. Approximately 80 Golgi stacks were analyzed and quantified per construct using specific criteria for vesicle size and attached versus unattached vesicles (*Materials and Methods*). The results show an increase in the number of unattached vesicles in the Rab14-S25N–GFP cells compared with cells expressing Rab14-wt–GFP and a similar number of attached vesicles with both constructs (Figure 4B). These results suggest that vesicles in Rab14-S25N–GFP-expressing cells are able to undergo both budding and fission from the Golgi/TGN membrane but are accumulating in the peri-Golgi region. Thus, Rab14 appears to be involved in the transport of vesicles between the Golgi and endosomes/plasma membrane.

Rab14 vesicles traffic to early endosomes and the plasma membrane

Because our EM data demonstrate an accumulation of vesicular membrane profiles in the vicinities of the Golgi apparatus, we next examined whether Rab14 is involved in the trafficking

of these vesicles. Because their flat morphology facilitates live cell imaging, we employed NRK cells expressing GFP-tagged Rab14 (Figure 5). We found that Rab14-wt–GFP-positive vesicles (Figure 5A) and Rab14-Q70L–GFP-positive vesicles (Figure 5B) move dynamically in the cell. In Rab14-wt–GFP cells, we observe vesicles exiting and entering the perinuclear region (Figure 5A and Video S1). In Rab14-Q70L cells, we observe vesicles undergoing fusion in the perinuclear region (Figure 5B and Video S2). Rab14-S25N–GFP localizes to an amorphous perinuclear compartment (Figure 5C) and, unlike Rab14-wt–GFP and Rab14-Q70L–GFP, we observe no vesicular movement of Rab14-S25N–GFP into or out of the Golgi region (Figure 5C and Video S3), suggesting that vesicles containing GFP–Rab14-S25N are held up at the Golgi/TGN level.

Our results suggest that Rab14 may regulate delivery of apically directed proteins between the TGN and apical endosomes or the plasma membrane. We next performed live cell imaging using MDCK cells expressing Rab14-wt–GFP and tetramethylrhodamine isothiocyanate (TRITC)-labeled ricin to mark the endocytic pathway. As shown in Figure 6A and in Video S4, vesicles containing Rab14 fuse with ricin-containing endosomes within 5 min of warming to 37°C. In addition, because not all the ricin is internalized within 5 min and continues to label the plasma membrane, Rab14-containing vesicles can be visualized fusing with the plasma membrane and then rebudding (Figure 6B and Video S5). These images indicate that Rab14 shuttles between early endosomes and the plasma membrane. Thus, Rab14 may regulate the trafficking of apically directed proteins by cycling between the TGN and early endosomes or the plasma membrane.

Rab14 is required for proper localization of the apical raft protein VIP/MAL

Because we saw a nucleotide-dependent interaction with VIP/MAL (Figure 1B), we next determined whether Rab14 could be involved in the targeting of this raft-associated molecule. As shown in Figure 7, in cells coexpressing Rab14-wt–GFP and VIP/MAL, VIP/MAL is targeted to the apical membrane and more importantly is not found intracellularly (section of VIP/MAL is in the middle of the cell) (Figure 7A). However, in cells expressing Rab14-S25N–GFP, there is a retention of VIP/MAL intracellularly (section of VIP/MAL is in the middle of the cell) and mis-targeting to the lateral membrane, as indicated by colocalizing with the basolateral marker, E-cadherin (Figure 7B).

Localization of Rab14 with the apical plasma membrane protein, gp135, or pIgA receptor

Recent results indicate that there are multiple pathways to the apical domain (33). To determine if Rab14 affects the trafficking of other apically associated membrane proteins, we looked at the well-established apical marker, gp135. When MDCK cells expressing Rab14-wt (Figure 8A, panel a), Rab14-Q70L (Figure 8A, panel b) or Rab14-S25N (Figure 8A, panel c) were labeled with antibodies against gp135, the distribution of gp135 was indistinguishable from untransfected cells (unpublished data). In addition, we also observe no alteration in the distribution of the polymeric immunoglobulin A (pIgA) receptor (Figure 8B) or the basolateral protein E-cadherin (Figure 8C) in cells expressing all Rab14 constructs. In addition, the trans-epithelial resistance of the cells was unaffected by the expression of any forms of Rab14 (unpublished data). Overall, these results suggest that Rab14 is selective for specific types of apical membrane proteins.

Rab14 localizes to recycling endosomes (29), and localization studies of transferrin and Rab14 suggest that these molecules exist in nearby domains (Figure 3C, panel c′). To further examine the specificity of the effects of Rab14 upon apical targeting and endosomal trafficking, we examined the effect of expression of GFP-tagged Rab14-wt, Rab14-Q70L and Rab14-S25N upon the recycling of basolaterally internalized transferrin. As shown in Figure 9, transferrin

recycling and transcytosis are unaffected by expression of any of these forms of Rab14, suggesting that Rab14 is not involved in the basolateral trafficking pathway.

Taken together, our results demonstrate a role for Rab14 in directing the trafficking of a subset of apical proteins in polarized epithelial cells.

Discussion

Loss of epithelial cell polarity has been associated with transformation and uncontrolled growth (34), and accurate delivery of newly synthesized proteins to both the apical and the basolateral membranes is necessary for normal epithelial cell function. Despite the wealth of information about sorting and delivery of newly synthesized proteins to the basolateral membrane (3,5, 15,21–25,35,36), the molecular hardware responsible for delivery of proteins and lipids to the apical domain remains largely uncharacterized. In this study, we report that the small GTPase Rab14 is involved in the polarized delivery of specific apical proteins from the TGN to the apical plasma membrane without affecting basolateral targeting or cell–cell junctions. We demonstrate that expression of the inactive form of Rab14 disrupts the TGN and causes missorting of an apical raft-associated protein, evidence that Rab14 regulates the trafficking of apical proteins. In addition, expression of GDP-bound Rab14 causes an increase in vesicles accumulating in the peri-Golgi region, suggesting that it is involved in transport of these vesicles.

How does Rab14 work? In MDCK cells, apically targeted molecules are sorted within the TGN by partitioning into domains through interactions with *N*-linked carbohydrates (7), GPI moieties (9) or the proteolipid MAL (16,17). These molecules presumably function to promote the formation of membrane domains, while other cytoplasmic machinery is required for the budding and delivery of these molecules and their cargo [but see Schuck and Simons (37)]. Although Rab proteins have been implicated in many steps of membrane trafficking (38), there are relatively few reports of Rab proteins binding to cargo molecules in the membrane. A notable example of a Rab protein binding to cargo is seen with the trafficking of pIgA receptor in the transcytotic pathway (39) where GTP-bound Rab3b inhibits transcytosis of the pIgA receptor. Rab21 also associates with the cytoplasmic domains of α-integrins, and nucleotide mutants of Rab21 affect association with and trafficking of β1-integrins (40). We have found that Rab14 interacts with the apical endosomal protein endotubin and VIP/MAL. Endotubin has been found to oligomerize and is highly *N*-glycosylated (41) and may serve as a scaffold for apical membrane proteins. Similar to Rab3b and Rab5a where the GTPase activity of the proteins controls their association with pIgA receptor or angiotensin 2-1A-receptor ($AT_{1A}R$) (39,42), respectively, the differential trafficking pathways for Rab14 could reflect the type of cargo Rab14 is transporting. Differential trafficking of apical proteins has been observed in the targeting of the raft-associated hemagglutinin and the non-raft-associated protein endolyn to apical compartments, suggesting that apical proteins traverse different endocytic intermediates on their way to the apical membrane in polarized cells (33). It may be that endotubin functions predominantly at the endosomal compartment, whereas VIP/MAL functions at the TGN. It is also possible that the difference in nucleotide-dependent binding of Rab14 with VIP/MAL reflects indirect binding and/or the presence of cofactors that modulate VIP/MAL binding to Rab14.

Subsets of Rab GTPases are expressed in the apical domain of epithelial cells and have been shown to regulate trafficking from endosomal compartments. Our colocalization and live cell imaging of Rab14 suggest that it cycles between the TGN, common and apical early endosomal compartments. In MDCK cells, in contrast with Rab14, Rab11a and Rab25 associate with the apical recycling endosome (ARE) and mutants of Rab11a and Rab25 selectively disrupt the apical recycling and transcytosis of IgA (43,44). Studies with Rab8 initially indicated that Rab8

regulates basolateral targeting through AP-1B adaptors in the recycling endosome (45). However, recent results in Rab8 knockout mice have implicated Rab8 in the trafficking of peptidases and transporters to the apical membrane of gut epithelial cells (46). This difference may reflect the different polarized trafficking pathways found in MDCK and intestinal epithelial cells (47–49). Finally, mutation of Rab4 caused trafficking of the transferrin receptor to the apical surface from the recycling endosome (50). However, transferrin recycling is unaffected by the overexpression of the Rab14 genotypes, suggesting that Rab14 is not involved in the targeting of basolateral proteins.

Rabs and their effectors work together to co-ordinate cargo sorting, budding, transport and fusion. To temporally and spatially control these cellular events between organelle compartments, Rabs must be highly organized to lend organelle specificity and function. This study demonstrates that Rab14 directs the trafficking of specific apical proteins in polarized epithelial cells. Future studies will determine other binding partners for Rab14 to characterize the regulation of these targeting events.

Materials and Methods

Reagents

Cell culture reagents were obtained from Gibco-BRL. The following antibodies were used: mouse anti-E-cadherin, rabbit anti-GFP and mouse anti-EEA1 (BD Biosciences), mouse anti-Golgi 58K protein, rabbit anti-FLAG and mouse γ-adaptin (Sigma-Aldrich, Inc.), mouse anti-gp135 (gift from Dr K. Matlin, University of Cincinnati, Cincinnati, OH, USA), mouse anti-endotubin (41), sheep anti-pIgA receptor (gift from Dr C. Okamoto, University of Southern California, Los Angeles, CA, USA), goat anti-dog transferrin (Bethyl Laboratories), mouse anti-clathrin heavy chain (Affinity Bioreagents Inc.) and Lysotracker (Invitrogen/Molecular Probes). Secondary antibodies were from Jackson ImmunoResearch Laboratories, Inc. TRITC–ricin was from EY Laboratories, Inc., and rhodamine and WGA–rhodamine (WGA–Rh) were from VECTOR Laboratories, Inc. All other chemicals and reagents were from Sigma-Aldrich Chemical Company.

Two-hybrid library screening and plasmid construction

Endotubin cytoplasmic domain (tail) bait was constructed by amplifying nucleotides 3620–3928 (amino acids 1160–1195) by PCR and subcloning into the GAL4-binding domain vector (pGBKT7, MATCHMAKER Library Construction kit; Clontech). This bait was used to screen a postnatal day 13 rat ileum complementary DNA library in GAL4-activating domain vector (pGADT7-Rec; Clontech). A total of 2×10^6 clones were screened following the manufacture's protocol. Positive colonies were sequenced and interactions confirmed by mating.

Full-length Rab14 was obtained by reverse transcriptase–polymerase chain reaction of mRNA obtained from neonatal rat ileum and subcloned into pEGFP-C2 vector (Clontech). The Q70L and S25N mutations were generated by site-directed mutagenesis using the Quik Change XL Mutagenesis Kit (Stratagene). For Rab14-Q70L, the primers were 5′–3′ GGATACGGCAGG-ACTCGAGCGATTTAGGG and 5′–3′ CCCTAAATCGCTCGAGTCCTGCCGTA-TCC. For Rab14-S25N, the primers were 5′–3′ GACATGGGAGTAAAAAA-TTGCTTGCTTCATC and 5′–3′ GATGAAGCAAGCAATTTTTTACTCCCATGTC. Endotubin cytoplasmic domain mutants for yeast two-hybrid studies were generated by site-directed mutagenesis of individual amino acids using the Quick Change XL Mutagenesis Kit as previously described (26). All mutations were verified by sequencing.

For GST pull-down experiments, full-length Rab14 was cloned into pET-41a (Novagen), and the CXC prenylation motif was deleted by PCR using the following primers: 5′–3′

GTGAACCCCAACCCCAGTGAGAAGGCTGTGG-CTGC and 3′–5′ GCAGCCACAGCCTTCTCACTGGGGTTGGGGTTCAC.

GST pull downs

Rab14–GST proteins were purified by sonication of bacterial cultures expressing the constructs followed by incubation of bacterial supernatants with Amersham Glutathione 4 Fast Flow beads for 1 h. Beads containing 100 μg of GST–Rab14 protein were incubated with 100 μM of either GTPγS or GDP and 2 mg of MDCK lysates expressing either VIP/MAL-FLAG or full-length endotubin. MDCK lysates were prepared using 1% TX-100, 150 mM NaCl, 5 mM ethylenediaminetetraacetic acid and 50 mM Tris, pH 7.5. After incubation, beads were washed and eluted in SDS–PAGE sample buffer.

Cell culture, immunofluorescent labeling and fluorescence microscopy

MDCK and NRK cells were transfected with Rab14–GFP constructs as previously described (26,51). MDCK cells expressing the Rab14 constructs were selected by growth in medium containing 400 μg/mL G418 for 10 days followed by colony selection. For experiments, cells were seeded onto Costar filters as previously described (26).

Prior to all experiments, MDCK cells were treated overnight with 4 mM butyric acid to induce expression of the transgenes, and for immunofluorescent labeling, cells were processed as previously described (52). For labeling with WGA–Rh, cells were fixed in 4% paraformaldehyde, permeabilized with 0.05% Nonidet P-40/PBS and incubated with 100 μg/mL WGA–Rh in PBS for 30 min at room temperature, washed with PBS and mounted with Aqua Poly/Mount (Polysciences, Inc.).

Images of cells on coverslips were acquired using the DeltaVision restoration microscopy system (Applied Precision, Inc.) using an Olympus IX70 inverted microscope (Olympus America, Inc.) and Photometrics-cooled charge-coupled device (CCD) camera (Roper Scientific Instruments); ×60 (1.4) or ×100 [numerical aperture (NA) 1.35] objectives were used to obtain the images. The *x*,*y* stacks were deconvolved using a Silicon Graphics Workstation (SGI) with measured point spread functions to create the final images. Cells on filters were imaged using a Zeiss LSM laser scanning system with a ×100 oil immersion objective, NA 1.4. Simultaneous two- or three-channel recording was performed using excitation wavelengths of 488, 533 and/or 633 nm through a *z*-stack of 10–50 μm in thickness. Images were processed and merged using ADOBE PHOTOSHOP software (Adobe Systems). To facilitate comparison, identical imaging and processing parameters were used for all figures. Intensity of intracellular fluorescence was measured using IMAGEJ (National Institutes of Health, NIH).

Transmission electron microscopy and Golgi vesicle quantification

MDCK cells stably expressing Rab14-wt or -S25N were grown as described above. For EM, cells were fixed in 3% glutaraldehyde/0.1 M cacodylate buffer, pH 7.2, and embedded in Spurrs resin (Electron Microscopy Sciences). Sections were examined using a Philips 410STEM at 80 kV, and images were acquired using a AMT-XR40 (Advanced Microscopy Techniques) digital camera.

To quantify the attached and unattached vesicles surrounding Golgi apparatus, 80 stacks were analyzed using IMAGEJ (NIH). The criteria used to define the vesicles around the Golgi were (i) vesicles must be less than 300 nm in diameter, (ii) vesicles must be within 0.5 μm of the Golgi stacks, (iii) vesicles where cytoplasm was present between the vesicle and the Golgi membrane were considered unattached and (iv) vesicles that appeared to rest upon the

membrane or to have a neck are considered attached. Statistical analysis was performed using Student's *t*-test.

Live cell imaging

Twenty-four hours after transfection, NRK cells expressing the Rab14–GFP constructs (wt, Q70L and S25N) were placed in live cell imaging media (DMEM-phenol red free, 10% FBS, 25 mM HEPES) and transferred to a closed viewing chamber equipped with an objective heat collar and a temperature-controlled air blower. Samples were maintained at 37°C and imaged using a ×100 oil objective and an Intelligent Innovations imaging system (Intelligent Imaging Innovations) with a Zeiss Axiovert 200M including a 175 Watt Xenon light source with a dual galvanometric filter changer, a Coolsnap HQ interline CCD camera and an *x*,*y* motorized stage with harmonic drive *z*-focusing. Using an enhanced green fluorescent protein filter set, 70 frames were taken at 2 seconds per frame for a 2-min movie. Each movie series was projected onto a single *x*, *y* plane. Movies were made using slidebook software.

For live cell imaging of MDCK cells, cells were grown on coverslips (Bioptechs) designed to fit onto the Focht live-cell chamber apparatus (Bioptechs). Time-lapse series were acquired at 37°C on the Olympus IX70 microscope system described above. Exposure times were 400–500 milliseconds for each channel and time-lapse sequences of 6 seconds. Series were exported as QuickTime movies or as single TIFF files and processed in ADOBE PHOTOSHOP 6.0.

Uptake studies

For transferrin uptake studies, canine apo-transferrin was saturated with iron using iron–nitrilotriacetate chelate as described in Bates and Wernicke (53), run twice through a G-25 Sephadex column (Pharmacia Biotech) and dialyzed against 20 mM HEPES (pH 7.0) buffer to a final concentration of 1.5–3 mg/mL. This iron-saturated transferrin was iodinated to a specific activity of 5.0–9.0 × 10^6 c.p.m./μg using Iodogen tubes (Pierce). Unincorporated $Na^{125}I$ was removed with a G-25 Sephadex column.

The transferrin-recycling assay on filter-grown cells expressing Rab14-wt, Rab14-Q70L and Rab14-S25N were performed as previously described (54).

Supplementary Material

Refer to Web version on PubMed Central for supplementary material.

Acknowledgments

The authors thank Dr K. Matlin for providing the anti-gp135 antibody and Dr C. Okamoto for anti-pIgA receptor antibody and Dr M. Caplan for the VIP/MAL plasmid. This study was supported by NIH grants DK43329 (to J. M. W.).

References

1. Mostov K, Su T, ter Beest M. Polarized epithelial membrane traffic: conservation and plasticity. Nat Cell Biol 2003;5:287–293. [PubMed: 12669082]
2. Rodriguez-Boulan E, Kreitzer G, Musch A. Organization of vesicular trafficking in epithelia. Nat Rev Mol Cell Biol 2005;6:233–247. [PubMed: 15738988]
3. Folsch H, Ohno H, Bonifacino JS, Mellman I. A novel clathrin adaptor complex mediates basolateral targeting in polarized epithelial cells. Cell 1999;99:189–198. [PubMed: 10535737]
4. Folsch H, Pypaert M, Schu P, Mellman I. Distribution and function of AP-1 clathrin adaptor complexes in polarized epithelial cells. J Cell Biol 2001;152:595–606. [PubMed: 11157985]

5. Gan Y, McGraw TE, Rodriguez-Boulan E. The epithelial-specific adaptor AP1B mediates post-endocytic recycling to the basolateral membrane. Nat Cell Biol 2002;4:605–609. [PubMed: 12105417]
6. Roush DL, Gottardi CJ, Naim HY, Roth MG, Caplan MJ. Tyrosine-based membrane protein sorting signals are differentially interpreted by polarized Madin-Darby canine kidney and LLC-PK1 epithelial cells. J Biol Chem 1998;273:26862–26869. [PubMed: 9756932]
7. Benting JH, Rietveld AG, Simons K. N-Glycans mediate the apical sorting of a GPI-anchored, raft-associated protein in Madin-Darby canine kidney cells. J Cell Biol 1999;146:313–320. [PubMed: 10427087]
8. Yeaman C, Le Gall AH, Baldwin AN, Monlauzeur L, Le Bivic A, Rodriguez-Boulan E. The O-glycosylated stalk domain is required for apical sorting of neurotrophin receptors in polarized MDCK cells. J Cell Biol 1997;139:929–940. [PubMed: 9362511]
9. Brown DA, Rose JK. Sorting of GPI-anchored proteins to glycolipid-enriched membrane subdomains during transport to the apical cell surface. Cell 1992;68:533–544. [PubMed: 1531449]
10. Chuang JZ, Sung CH. The cytoplasmic tail of rhodopsin acts as a novel apical sorting signal in polarized MDCK cells. J Cell Biol 1998;142:1245–1256. [PubMed: 9732285]
11. Karim-Jimenez Z, Hernando N, Biber J, Murer H. Requirement of a leucine residue for (apical) membrane expression of type IIb NaPi cotransporters. Proc Natl Acad Sci U S A 2000;97:2916–2921. [PubMed: 10717004]
12. Gokay KE, Young RS, Wilson JM. Cytoplasmic signals mediate apical early endosomal targeting of endotubin in MDCK cells. Traffic 2001;2:487–500. [PubMed: 11422942]
13. Sarnataro D, Campana V, Paladino S, Stornaiuolo M, Nitsch L, Zurzolo C. PrP(C) association with lipid rafts in the early secretory pathway stabilizes its cellular conformation. Mol Biol Cell 2004;15:4031–4042. [PubMed: 15229281]
14. Schuck S, Manninen A, Honsho M, Fullekrug J, Simons K. Generation of single and double knockdowns in polarized epithelial cells by retrovirus-mediated RNA interference. Proc Natl Acad Sci U S A 2004;101:4912–4917. [PubMed: 15051873]
15. Lafont F, Verkade P, Galli T, Wimmer C, Louvard D, Simons K. Raft association of SNAP receptors acting in apical trafficking in Madin-Darby canine kidney cells. Proc Natl Acad Sci U S A 1999;96:3734–3738. [PubMed: 10097106]
16. Puertollano R, Martin-Belmonte F, Millan J, de Marco MC, Albar JP, Kremer L, Alonso MA. The MAL proteolipid is necessary for normal apical transport and accurate sorting of the influenza virus hemagglutinin in Madin-Darby canine kidney cells. J Cell Biol 1999;145:141–151. [PubMed: 10189374]
17. Cheong KH, Zacchetti D, Schneeberger EE, Simons K. VIP17/MAL, a lipid raft-associated protein, is involved in apical transport in MDCK cells. Proc Natl Acad Sci U S A 1999;96:6241–6248. [PubMed: 10339572]
18. Vieira OV, Verkade P, Manninen A, Simons K. FAPP2 is involved in the transport of apical cargo in polarized MDCK cells. J Cell Biol 2005;170:521–526. [PubMed: 16103222]
19. Kreitzer G, Schmoranzer J, Low SH, Li X, Gan Y, Weimbs T, Simon SM, Rodriguez-Boulan E. Three-dimensional analysis of post-Golgi carrier exocytosis in epithelial cells. Nat Cell Biol 2003;5:126–136. [PubMed: 12545172]
20. Keller P, Toomre D, Diaz E, White J, Simons K. Multicolour imaging of post-Golgi sorting and trafficking in live cells. Nat Cell Biol 2001;3:140–149. [PubMed: 11175746]
21. Folsch H, Pypaert M, Maday S, Pelletier L, Mellman I. The AP-1A and AP-1B clathrin adaptor complexes define biochemically and functionally distinct membrane domains. J Cell Biol 2003;163:351–362. [PubMed: 14581457]
22. Grindstaff KK, Yeaman C, Anandasabapathy N, Hsu SC, Rodriguez-Boulan E, Scheller RH, Nelson WJ. Sec6/8 complex is recruited to cell-cell contacts and specifies transport vesicle delivery to the basal-lateral membrane in epithelial cells. Cell 1998;93:731–740. [PubMed: 9630218]
23. Low SH, Chapin SJ, Wimmer C, Whiteheart SW, Komuves LG, Mostov KE, Weimbs T. The SNARE machinery is involved in apical plasma membrane trafficking in MDCK cells. J Cell Biol 1998;141:1503–1513. [PubMed: 9647644]

24. Low SH, Chapin SJ, Weimbs T, Komuves LG, Bennett MK, Mostov KE. Differential localization of syntaxin isoforms in polarized Madin-Darby canine kidney cells. Mol Biol Cell 1996;7:2007–2018. [PubMed: 8970161]
25. Musch A, Cohen D, Kreitzer G, Rodriguez-Boulan E. cdc42 regulates the exit of apical and basolateral proteins from the trans-Golgi network. EMBO J 2001;20:2171–2179. [PubMed: 11331583]
26. Gokay KE, Wilson JM. Targeting of an apical endosomal protein to endosomes in Madin-Darby canine kidney cells requires two sorting motifs. Traffic 2000;1:354–365. [PubMed: 11208120]
27. Brown PS, Wang E, Aroeti B, Chapin SJ, Mostov KE, Dunn KW. Definition of distinct compartments in polarized Madin-Darby canine kidney (MDCK) cells for membrane-volume sorting, polarized sorting and apical recycling. Traffic 2000;1:124–140. [PubMed: 11208093]
28. Wang E, Brown PS, Aroeti B, Chapin SJ, Mostov KE, Dunn KW. Apical and basolateral endocytic pathways of MDCK cells meet in acidic common endosomes distinct from a nearly-neutral apical recycling endosome. Traffic 2000;1:480–493. [PubMed: 11208134]
29. Junutula JR, De Maziere AM, Peden AA, Ervin KE, Advani RJ, van Dijk SM, Klumperman J, Scheller RH. Rab14 is involved in membrane trafficking between the Golgi complex and endosomes. Mol Biol Cell 2004;15:2218–2229. [PubMed: 15004230]
30. Kyei GB, Vergne I, Chua J, Roberts E, Harris J, Junutula JR, Deretic V. Rab14 is critical for maintenance of Mycobacterium tuberculosis phagosome maturation arrest. EMBO J 2006;25:5250–5259. [PubMed: 17082769]
31. Teuchert M, Schafer W, Berghofer S, Hoflack B, Klenk HD, Garten W. Sorting of furin at the trans-Golgi network. Interaction of the cytoplasmic tail sorting signals with AP-1 Golgi-specific assembly proteins. J Biol Chem 1999;274:8199–8207. [PubMed: 10075724]
32. Gonatas NK, Kim SU, Stieber A, Avrameas S. Internalization of lectins in neuronal GERL. J Cell Biol 1977;73:1–13. [PubMed: 856827]
33. Cresawn KO, Potter BA, Oztan A, Guerriero CJ, Ihrke G, Goldenring JR, Apodaca G, Weisz OA. Differential involvement of endocytic compartments in the biosynthetic traffic of apical proteins. EMBO J 2007;26:3737–3748. [PubMed: 17673908]
34. Bilder D, Li M, Perrimon N. Cooperative regulation of cell polarity and growth by Drosophila tumor suppressors. Science 2000;289:113–116. [PubMed: 10884224]
35. Simmen T, Honing S, Icking A, Tikkanen R, Hunziker W. AP-4 binds basolateral signals and participates in basolateral sorting in epithelial MDCK cells. Nat Cell Biol 2002;4:154–159. [PubMed: 11802162]
36. Yeaman C, Ayala MI, Wright JR, Bard F, Bossard C, Ang A, Maeda Y, Seufferlein T, Mellman I, Nelson WJ, Malhotra V. Protein kinase D regulates basolateral membrane protein exit from trans-Golgi network. Nat Cell Biol 2004;6:106–112. [PubMed: 14743217]
37. Schuck S, Simons K. Polarized sorting in epithelial cells: raft clustering and the biogenesis of the apical membrane. J Cell Sci 2004;117:5955–5964. [PubMed: 15564373]
38. Zerial M, McBride H. Rab proteins as membrane organizers. Nat Rev Mol Cell Biol 2001;2:107–117. [PubMed: 11252952]
39. van ISC, Tuvim MJ, Weimbs T, Dickey BF, Mostov KE. Direct interaction between Rab3b and the polymeric immunoglobulin receptor controls ligand-stimulated transcytosis in epithelial cells. Dev Cell 2002;2:219–228. [PubMed: 11832247]
40. Pellinen T, Arjonen A, Vuoriluoto K, Kallio K, Fransen JA, Ivaska J. Small GTPase Rab21 regulates cell adhesion and controls endosomal traffic of beta1-integrins. J Cell Biol 2006;173:767–780. [PubMed: 16754960]
41. Wilson JM, Whitney JA, Neutra MR. Identification of an endosomal antigen specific to absorptive cells of suckling rat ileum. J Cell Biol 1987;105:691–703. [PubMed: 3305521]
42. Seachrist JL, Laporte SA, Dale LB, Babwah AV, Caron MG, Anborgh PH, Ferguson SS. Rab5 association with the angiotensin II type 1A receptor promotes Rab5 GTP binding and vesicular fusion. J Biol Chem 2002;277:679–685. [PubMed: 11682489]
43. Casanova JE, Wang X, Kumar R, Bhartur SG, Navarre J, Woodrum JE, Altschuler Y, Ray GS, Goldenring JR. Association of Rab25 and Rab11a with the apical recycling system of polarized Madin-Darby canine kidney cells. Mol Biol Cell 1999;10:47–61. [PubMed: 9880326]

44. Wang X, Kumar R, Navarre J, Casanova JE, Goldenring JR. Regulation of vesicle trafficking in madin-darby canine kidney cells by Rab11a and Rab25. J Biol Chem 2000;275:29138–29146. [PubMed: 10869360]
45. Ang AL, Folsch H, Koivisto UM, Pypaert M, Mellman I. The Rab8 GTPase selectively regulates AP-1B-dependent basolateral transport in polarized Madin-Darby canine kidney cells. J Cell Biol 2003;163:339–350. [PubMed: 14581456]
46. Sato T, Mushiake S, Kato Y, Sato K, Sato M, Takeda N, Ozono K, Miki K, Kubo Y, Tsuji A, Harada R, Harada A. The Rab8 GTPase regulates apical protein localization in intestinal cells. Nature 2007;448:366–369. [PubMed: 17597763]
47. Matter K, Stieger B, Klumperman J, Ginsel L, Hauri HP. Endocytosis, recycling, and lysosomal delivery of brush border hydrolases in cultured human intestinal epithelial cells (Caco-2). J Biol Chem 1990;265:3503–3512. [PubMed: 1968064]
48. Rindler MJ, Traber MG. A specific sorting signal is not required for the polarized secretion of newly synthesized proteins from cultured intestinal epithelial cells. J Cell Biol 1988;107:471–479. [PubMed: 2458357]
49. Traber MG, Kayden HJ, Rindler MJ. Polarized secretion of newly synthesized lipoproteins by the Caco-2 human intestinal cell line. J Lipid Res 1987;28:1350–1363. [PubMed: 3430064]
50. Mohrmann K, Leijendekker R, Gerez L, van Der Sluijs P. rab4 regulates transport to the apical plasma membrane in Madin-Darby canine kidney cells. J Biol Chem 2002;277:10474–10481. [PubMed: 11790789]
51. Wilson JM, Colton TL. Targeting of an intestinal apical endosomal protein to endosomes in nonpolarized cells. J Cell Biol 1997;136:319–330. [PubMed: 9015303]
52. Hernandez-Deviez DJ, Roth MG, Casanova JE, Wilson JM. ARNO and ARF6 regulate axonal elongation and branching through downstream activation of phosphatidylinositol 4-phosphate 5-kinase {alpha}. Mol Biol Cell 2004;15:111–120. [PubMed: 14565977]
53. Bates GW, Wernicke J. The kinetics and mechanism of iron(3) exchange between chelates and transferrin. IV. The reaction of transferrin with iron(3) nitrilotriacetate. J Biol Chem 1971;246:3679–3685. [PubMed: 5578914]
54. Leung SM, Rojas R, Maples C, Flynn C, Ruiz WG, Jou TS, Apodaca G. Modulation of endocytic traffic in polarized Madin-Darby canine kidney cells by the small GTPase RhoA. Mol Biol Cell 1999;10:4369–4384. [PubMed: 10588664]

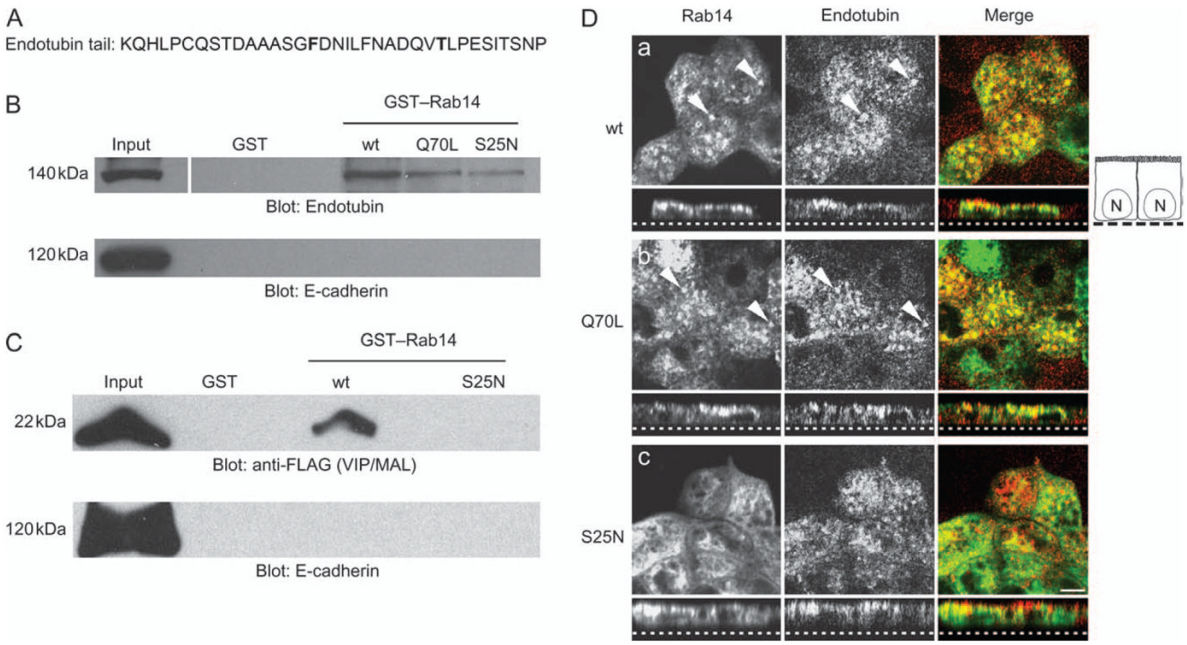

Figure 1. Endotubin and VIP/MAL interact with the small GTPase Rab14

A) Endotubin cytoplasmic domain used for bait construction. Motifs critical for apical endosomal targeting are indicated in bold. B) Rab14–GST (wt, Q70L and S25N)-tagged proteins were used to pull down endotubin or VIP/MAL from MDCK cells followed by immunoblotting. Results show that binding of full-length endotubin to Rab14 is not nucleotide dependent (B). However, binding of VIP/MAL is nucleotide dependent (C). None of the Rab14–GST constructs interacts with the basolateral marker, E-cadherin. Input is 5% of total. D) MDCK cells expressing Rab14-wt, -Q70L, or -S25N–GFP (green) and endotubin (red) were visualized by confocal microscopy. Coexpression of Rab14-wt and endotubin resulted in areas of overlap in the apical domain (arrowheads). Rab14-Q70L and endotubin also show extensive colocalization (arrowheads). Coexpression of Rab14-S25N and endotubin resulted in some areas of colocalization as well as a nonpolarized distribution of Rab14-S25N. Dotted line in the *z*-stack represents the bottom of the filter. Scale bar, 5 μm.

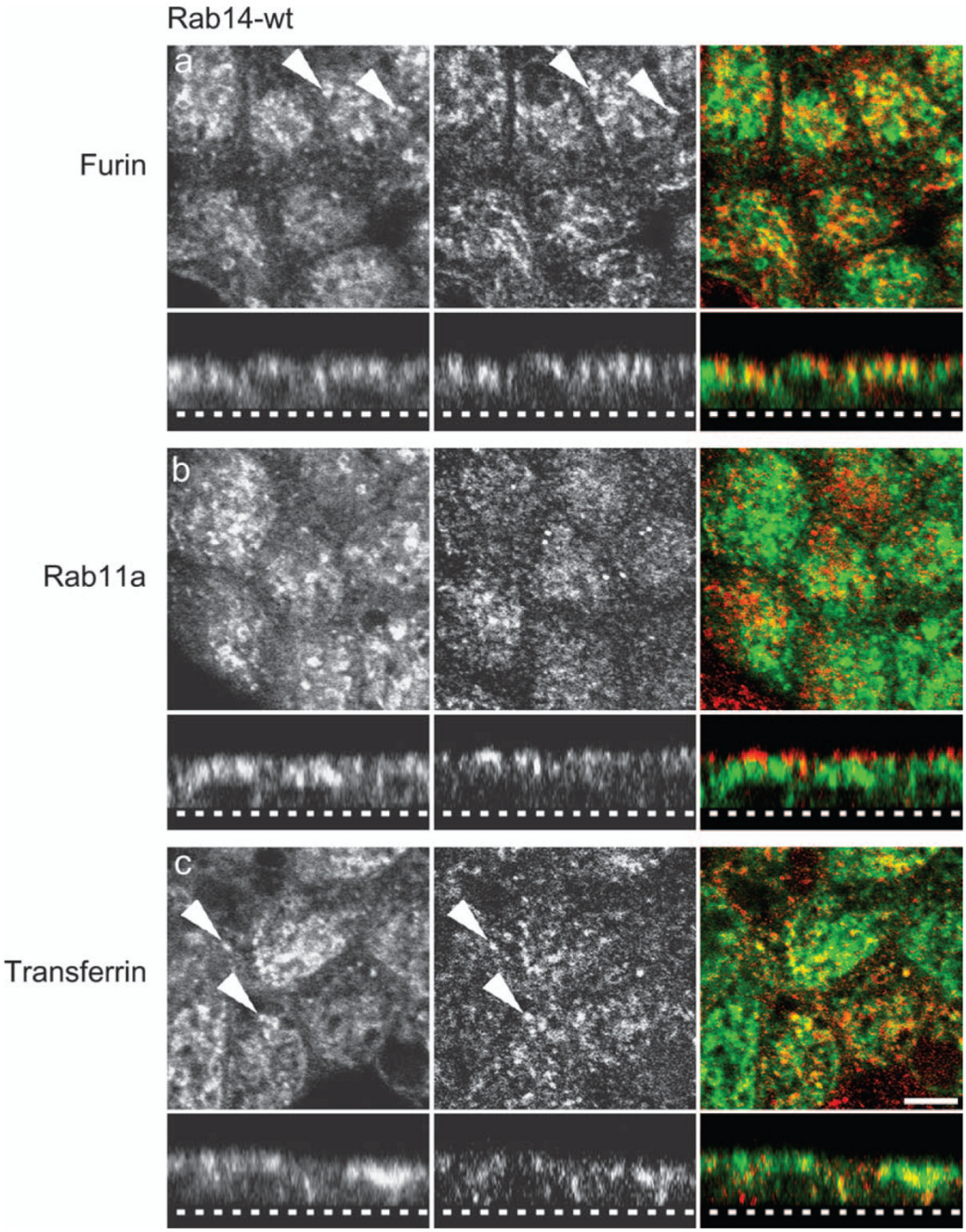

Figure 2. Subcellular localization of Rab14 in polarized epithelial cells

MDCK cells stably expressing Rab14-wt–GFP were labeled with anti-furin (A, red), anti-Rab11a (B, red) or anti-transferrin receptor (C, red) and visualized by confocal microscopy. There is some colocalization of Rab14-wt–GFP with furin (TGN) and transferrin receptor (common endosome) (arrowheads). No colocalization was observed with the ARE marker, Rab11a. Dotted line in the *z*-stack represents the bottom of the filter. Scale bar, 5 μm.

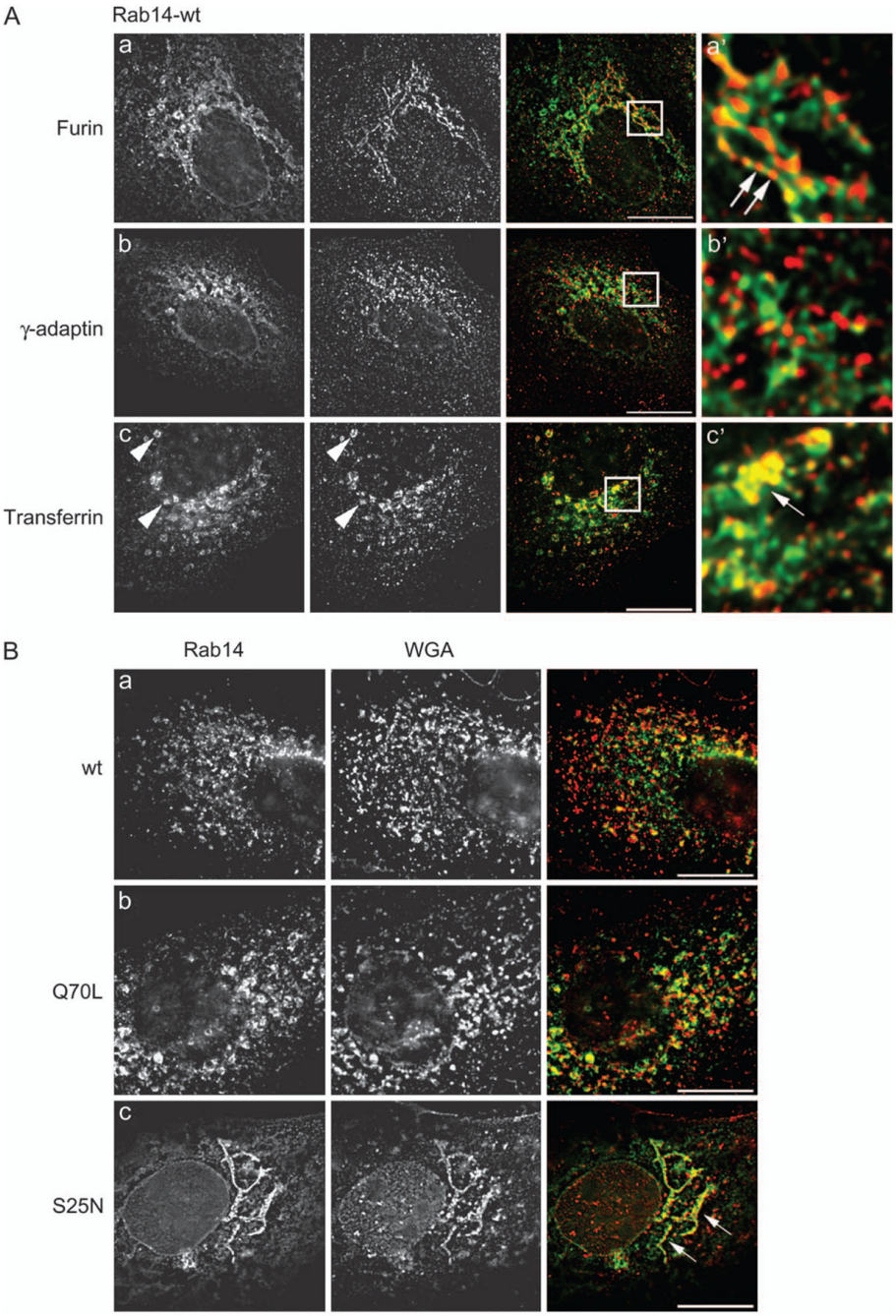

Figure 3. Subcellular localization of Rab14 in nonpolarized epithelial cells

A) MDCK cells transfected with Rab14-wt–GFP (green), labeled with anti-furin (panel a, red), anti-γ-adaptin (panel b, red) or anti-transferrin receptor (panel c, red) and visualized by deconvolution microscopy. Rab14 and furin (arrows, panel a′) are present in adjacent membrane domains. There is also some colocalization with the transferrin receptor (arrow and arrowheads, panels c′ and c) but no colocalization with γ-adaptin (panel b′). B) Expression of Rab14-wt (B, panel a) or Rab14-Q70L–GFP (B, panel b) did not affect the structure of the TGN, labeled in this study with WGA–Rh. In contrast, expression of Rab14-S25N caused a dramatic expansion and reorganization of the TGN with extensive overlay of the labels (B, panel c, arrows). Scale bars, 10 μm.

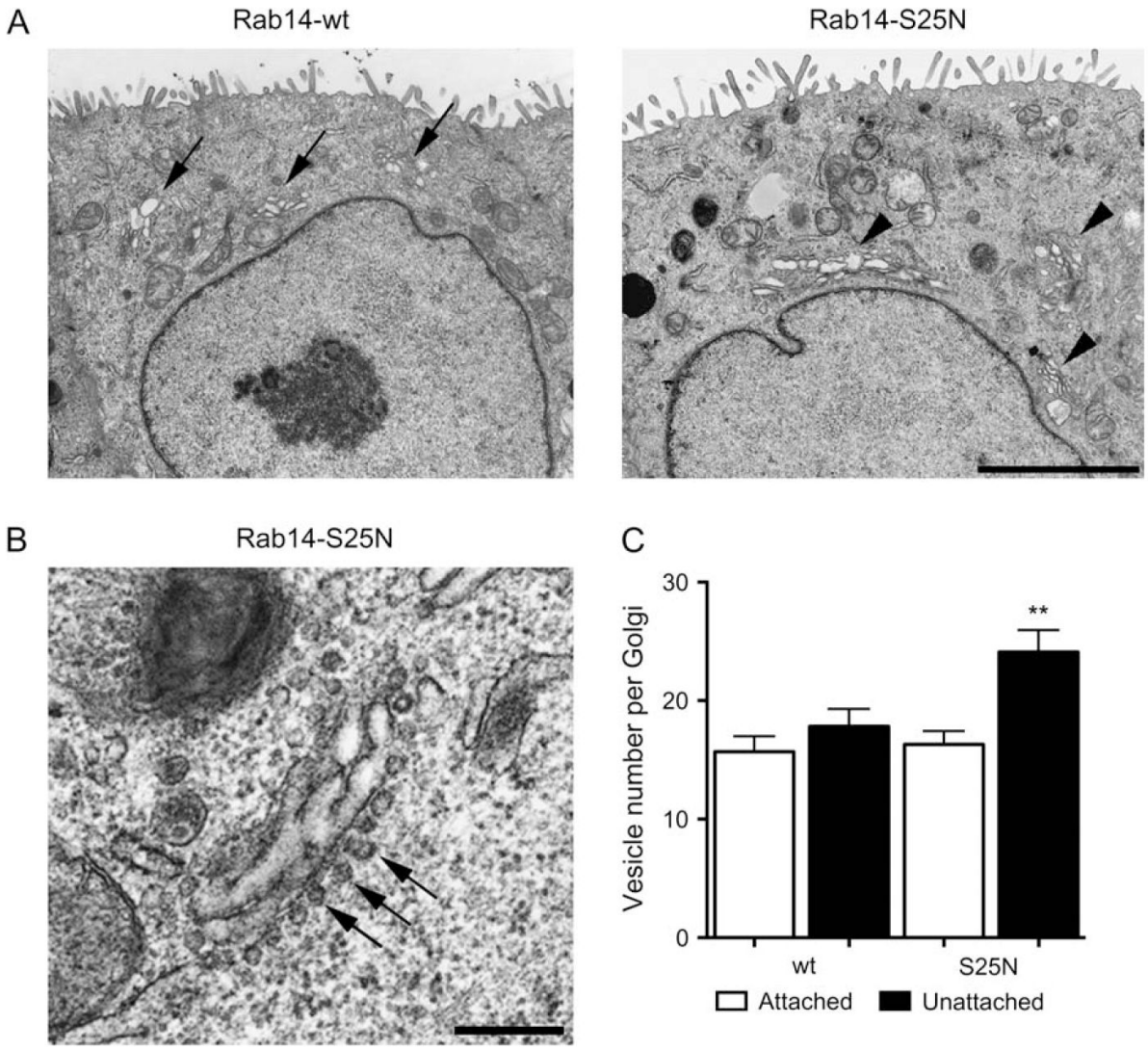

Figure 4. Rab14 is not involved in budding/fission of vesicles from the TGN

Low magnification of cells expressing Rab14-wt and Rab14-S25N. Cells expressing Rab14-wt display normal Golgi morphology (arrows, A – left panel) compared with Rab14-S25N-expressing cells (arrowheads, A – right panel) where Golgi membranes are expanded. B) High magnification of a Golgi region in cells expressing Rab14-S25N demonstrates an increase in vesicles lined up at the Golgi membrane (arrows). Scale bar, 0.5 μm. C) Rab14-S25N-expressing cells have a significant increase in unattached vesicles in the peri-Golgi compared with Rab14-wt (**$p < 0.005$).

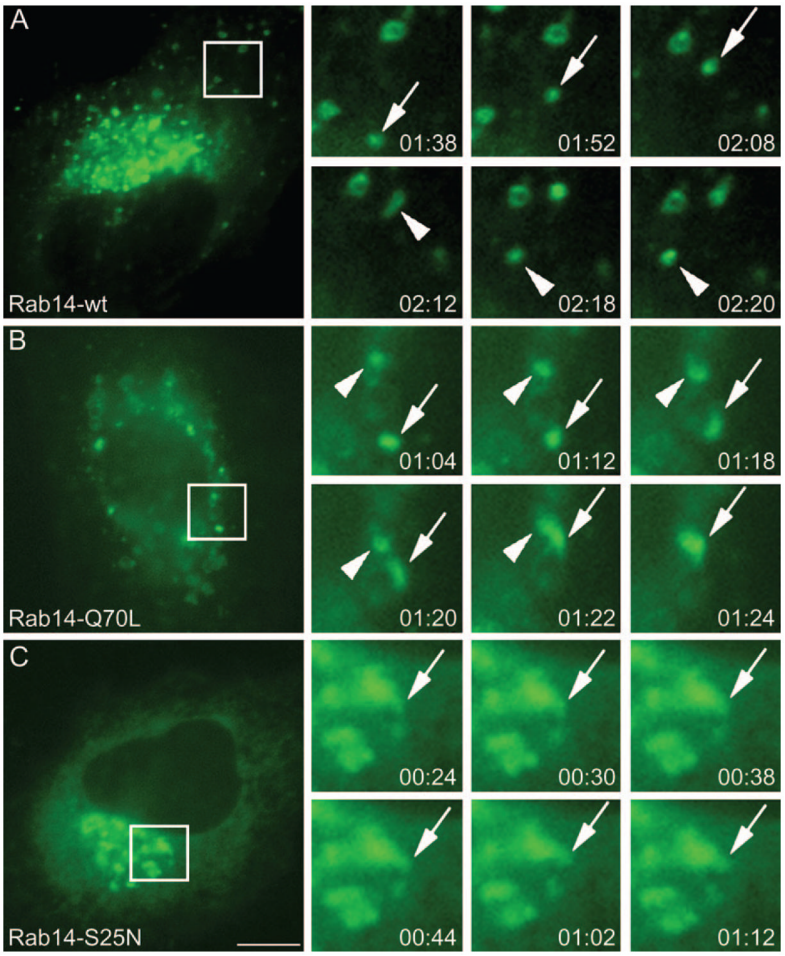

Figure 5. Nucleotide states determine motility of Rab14 vesicles

NRK cells expressing Rab14-wt, -Q70L and -S25N–GFP were imaged by live cell fluorescence microscopy. Selected frames from time-lapse images were enlarged and vesicles tracked. Individual frames were taken for 2 min and 20 seconds for each Rab14 construct. (A) Rab14-wt vesicles traffic in and out of the perinuclear region; time lapse shows a vesicle undergoing anterograde transport from the perinuclear region (arrow) and then undergoing retrograde movement (arrowheads). (B) Rab14-Q70L vesicles undergo fusion into the perinuclear region; time lapse shows a vesicle undergoing fusion (arrow) with another vesicle (arrowhead) in the perinuclear region. In contrast, cells expressing (C) Rab14-S25N display no vesicle movement and membrane structures containing Rab14 remain constant (arrows). The time is shown in min:seconds. Scale bar, 10 μm.

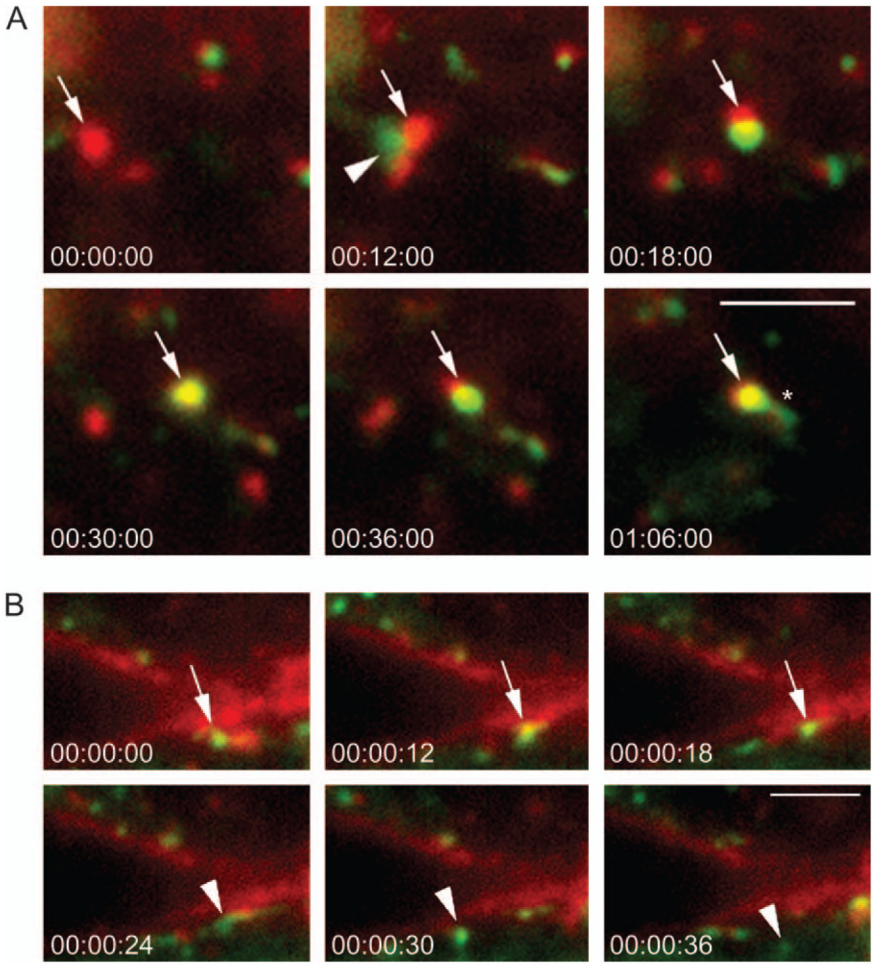

Figure 6. Rab14-wt vesicles traffic to early endosomes and plasma membrane

Rab14-wt–GFP (green)-expressing cells were incubated with ricin–TRITC (red) at 4°C and warmed to 37°C. Image acquisition was initiated within 5 min of warming. Individual frames were taken over a 10-min period (see supplementary material videos 4 and 5). A) Rab14-wt–GFP-containing vesicle (arrowhead) docks and fuses with an ricin–TRITC-labeled early endosome (arrow), and subsequently, a Rab14 tubular structure emerges from the vesicle (asterisk in 01:06:00). B) Rab14 vesicle (arrow) is docked at the ricin–TRITC-labeled plasma membrane; additional frames indicate the vesicle fusing with the plasma membrane. The Rab14-wt–GFP-positive vesicle then buds off the plasma membrane and moves into the cytoplasm (arrowhead in 00:00:24). The Rab14-wt–GFP domain then buds off from the plasma membrane (arrowhead in 00:30:00 and 00:36:00). The time is shown in min:seconds:milliseconds. Scale bars, A–B, 2.5 μm.

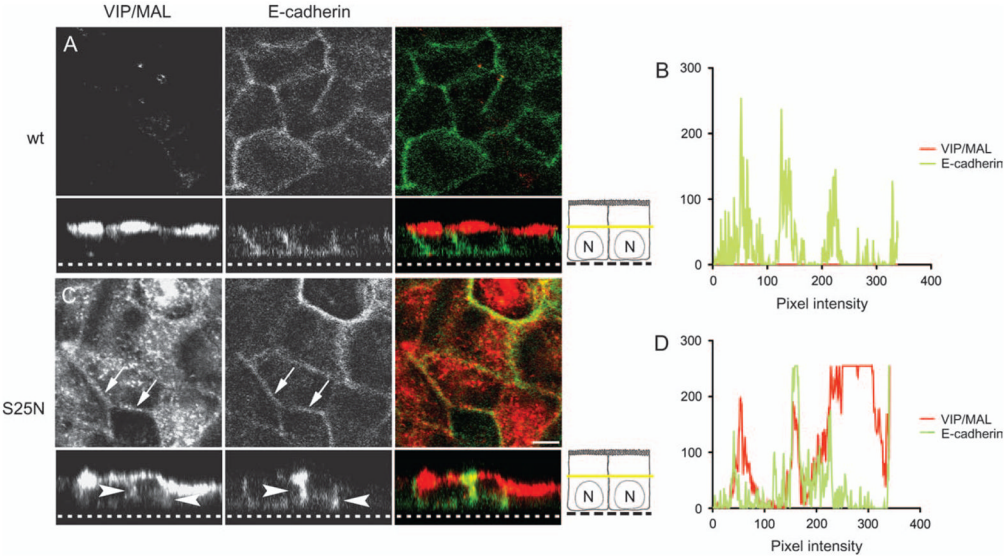

Figure 7. Inactive Rab14 selectively disrupts targeting of the raft-associated protein VIP/MAL

Cells expressing Rab14-wt or Rab14-S25N and VIP/MAL were labeled and examined by confocal microscopy. The plane of section in the *x–y* images is indicated by the yellow bar in the cartoon. A) Cells expressing Rab14-wt demonstrate an apical distribution of VIP/MAL, with no labeling in the subapical cytoplasm. No colocalization is observed with E-cadherin. B) Measurement of pixel intensity demonstrates no colocalization with E-cadherin. C) In cells expressing Rab14-S25N, VIP/MAL is retained intracellularly and localizes to the basolateral membrane shown by the colocalization with E-cadherin (arrows and arrowheads). D) Measurement of pixel intensity demonstrates extensive overlay between the two signals. Note: Rab14 is not shown in these images. Dotted line in the *z*-stack represents the bottom of the filter. Scale bar, 5 μm.

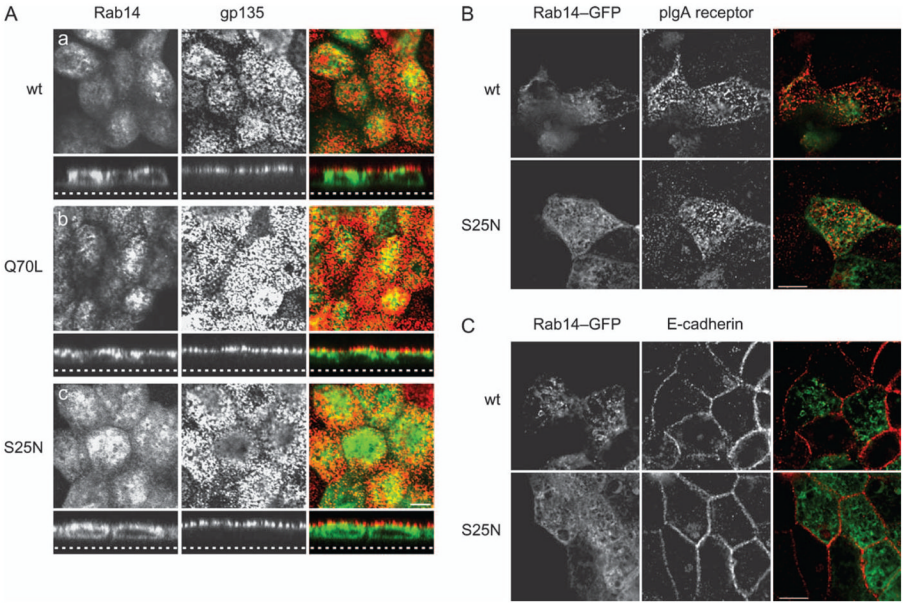

Figure 8. Rab14 does not affect the targeting of the apical proteins, gp135 and pIgA receptor

A) Cells expressing Rab14-wt, Rab14-Q70L and Rab14-S25N have an apical distribution of gp135 (red, a, b and c). B) The distribution of the pIgA receptor and C) E-cadherin was also unaffected by all forms of Rab14. Dotted line in the *z*-stack represents the bottom of the filter. Scale bars, 5 μm.

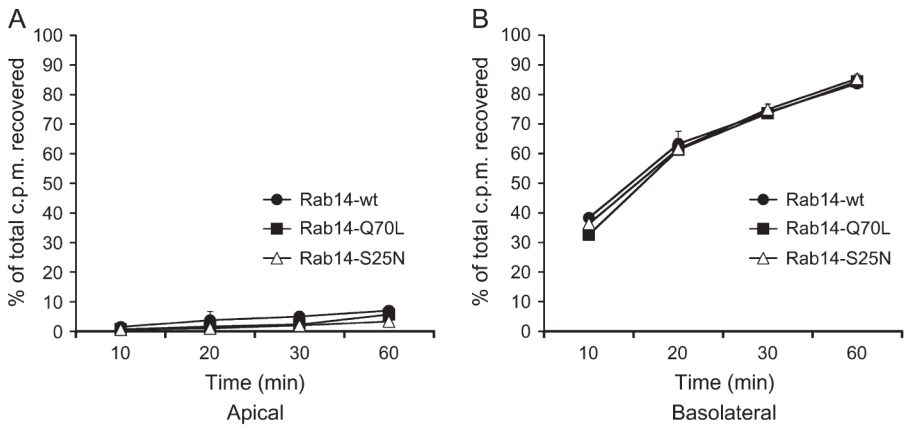

Figure 9. Rab14 has no effect on basolateral recycling of transferrin

Polarized epithelial cells expressing wt- (filled circles), Q70L-(filled squares) or S25N-Rab14 (open triangles) were loaded with ^{125}I-labeled transferrin from the basolateral side of the monolayer. Apical (A) and basolateral (B) media were harvested at different time-points to assess basolateral recycling and basolateral-to-apical transcytosis, respectively. Data are presented as mean (±SD) percentage of counts per minute recovered for each condition.

Table 1

Rab14 does not interact with endotubin mutants that are mistargeted basolaterally[a]

	Cytoplasmic domain sequence	Targeting	Interaction with Rab14
wt	KQHLPCQSTDAAASGFDNILFNADQVTLPESITSNP	A	+
F1180A	KQHLPCQSTDAAASGFDNILANADQVTLPESITSNP	A	+
T1186A	KQHLPCQSTDAAASGFDNILFNADQVALPESITSNP	A	+
F1180A/T1186A	KQHLPCQSTDAAASGFDNILANADQVALPESITSNP	B	−

[a]The cytoplasmic domain of endotubin and mutations of F1180A (hydrophobic motif) and T1186A (CKII site) are targeted to the apical domain (26) and interact with Rab14 in the yeast two-hybrid system. However, the double mutant T1186A/F1180A is mistargeted to the basolateral membrane (26) and showed no interaction with Rab14 in the yeast two-hybrid system.